

University of Wollongong  
**Research Online**

---

Illawarra Health and Medical Research Institute

Faculty of Science, Medicine and Health

---

1-1-2017

**In vivo and in vitro testing of native  $\alpha$ -conotoxins from the injected venom of *Conus purpurascens***

Mickelene Hoggard

*US National Institute of Standards and Technology, Florida Atlantic University*

Alena Rodriguez

*Florida Atlantic University*

Hermínsul Cano

*Florida Atlantic University*

Evan Clark

*Florida Atlantic University*

Han Shen Tae

*University of Wollongong, [hstae@uow.edu.au](mailto:hstae@uow.edu.au)*

*See next page for additional authors*

Follow this and additional works at: <https://ro.uow.edu.au/ihmri>

 Part of the [Medicine and Health Sciences Commons](#)

---

**Recommended Citation**

Hoggard, Mickelene; Rodriguez, Alena; Cano, Hermínsul; Clark, Evan; Tae, Han Shen; Adams, David J.; Godenschwege, Tanja A.; and Marí, Frank, "In vivo and in vitro testing of native  $\alpha$ -conotoxins from the injected venom of *Conus purpurascens*" (2017). *Illawarra Health and Medical Research Institute*. 1150. <https://ro.uow.edu.au/ihmri/1150>

Research Online is the open access institutional repository for the University of Wollongong. For further information contact the UOW Library: [research-pubs@uow.edu.au](mailto:research-pubs@uow.edu.au)

---

## In vivo and in vitro testing of native $\alpha$ -conotoxins from the injected venom of *Conus purpurascens*

### Abstract

$\alpha$ -Conotoxins inhibit nicotinic acetylcholine receptors (nAChRs) and are used as probes to study cholinergic pathways in vertebrates. Model organisms, such as *Drosophila melanogaster*, express nAChRs in their CNS that are suitable to investigate the neuropharmacology of  $\alpha$ -conotoxins *in vivo*. Here we report the paired nanoinjection of native  $\alpha$ -conotoxin PIA and two novel  $\alpha$ -conotoxins, PIC and PIC[07], from the injected venom of *Conus purpurascens* and electrophysiological recordings of their effects on the giant fiber system (GFS) of *D. melanogaster* and heterologously expressed nAChRs in *Xenopus* oocytes.  $\alpha$ -PIA caused disruption of the function of giant fiber dorsal longitudinal muscle (GF-DLM) pathway by inhibiting the D $\alpha$ 7 nAChR a homolog to the vertebrate  $\alpha$ 7 nAChR, whereas PIC and PIC[07] did not. PIC and PIC[07] reversibly inhibited ACh-evoked currents mediated by vertebrate rodent (r) $\alpha$ 1 $\beta$ 1 $\delta$  $\gamma$ ,  $\alpha$ 1 $\beta$ 1 $\delta$  $\epsilon$  and human (h) $\alpha$ 3 $\beta$ 2, but not h $\alpha$ 7 nAChR subtypes expressed in *Xenopus* oocytes with the following selectivity: r $\alpha$ 1 $\beta$ 1 $\delta$  $\epsilon$  > r $\alpha$ 1 $\beta$ 1 $\delta$  $\gamma$   $\approx$  h $\alpha$ 3 $\beta$ 2 > > h $\alpha$ 7. Our study emphasizes the importance of loop size and  $\alpha$ -conotoxin sequence specificity for receptor binding. These studies can be used for the evaluation of the neuropharmacology of novel  $\alpha$ -conotoxins that can be utilized as molecular probes for diseases such as, Alzheimer's, Parkinson's, and cancer.

### Disciplines

Medicine and Health Sciences

### Publication Details

Hoggard, M. F., Rodriguez, A. M., Cano, H., Clark, E., Tae, H., Adams, D. J., Godenschwege, T. A. & Mari, F. (2017). *In vivo* and *in vitro* testing of native  $\alpha$ -conotoxins from the injected venom of *Conus purpurascens*. *Neuropharmacology*, 127 253-259.

### Authors

Mickelene Hoggard, Alena Rodriguez, Herminsul Cano, Evan Clark, Han Shen Tae, David J. Adams, Tanja A. Godenschwege, and Frank Mari

## ***In vivo* and *in vitro* testing of native $\alpha$ -conotoxins from the injected venom of *Conus purpurascens***

Mickelene F. Hoggard<sup>1,2†</sup>, Alena M. Rodriguez<sup>3†</sup>, Herminsul Cano<sup>2</sup>, Evan Clark<sup>2</sup>, Han-Shen Tae<sup>4</sup>, David J. Adams<sup>4</sup>, Tanja A. Godenschwege<sup>5</sup>, Frank Mari<sup>1,2\*</sup>

<sup>1</sup>Marine Biochemical Sciences, Chemical Sciences Division, National Institute of Standards and Technology, 331 Fort Johnson Road, Charleston, SC, 29412, USA, <sup>2</sup>Department of Chemistry and Biochemistry, <sup>3</sup>Department of Biomedical Science, Florida Atlantic University, 777 Glades Road, Boca Raton, FL 33431-0991, USA, <sup>4</sup>Illawarra Health and Medical Research Institute (IHMRI), University of Wollongong, Wollongong, NSW 2522, Australia, and <sup>5</sup>Department of Biological Sciences, Florida Atlantic University, 777 Glades Road, Boca Raton, FL 33431-0991, USA.

†These authors contributed equally

\*Corresponding Author: Tel.: +1 (843) 725-4821. E-mail: frank.mari@nist.gov

**ABSTRACT:**  $\alpha$ -Conotoxins inhibit nicotinic acetylcholine receptors (nAChRs) and are used as probes to study cholinergic pathways in vertebrates. Model organisms, such as *Drosophila melanogaster*, express nAChRs in their CNS that are suitable to investigate the neuropharmacology of  $\alpha$ -conotoxins *in vivo*. Here we report the paired nanoinjection of native  $\alpha$ -conotoxin PIA and two novel  $\alpha$ -conotoxins, PIC and PIC[O7], from the injected venom of *Conus purpurascens* and electrophysiological recordings of their effects on the giant fiber system (GFS) of *D. melanogaster* and heterologously expressed nAChRs in *Xenopus* oocytes.  $\alpha$ -PIA caused disruption of the function of giant fiber dorsal longitudinal muscle (GF-DLM) pathway by inhibiting the D $\alpha$ 7 nAChR a homolog to the vertebrate  $\alpha$ 7 nAChR, whereas PIC and PIC[O7] did not. PIC and PIC[O7] inhibited ACh-evoked currents mediated by vertebrate rodent (r) $\alpha$ 1 $\beta$ 1 $\delta$  $\gamma$ , r $\alpha$ 1 $\beta$ 1 $\delta$  $\epsilon$  and human (h) $\alpha$ 3 $\beta$ 2, but not h $\alpha$ 7 nAChR subtypes expressed in *Xenopus* oocytes with the following selectivity: r $\alpha$ 1 $\beta$ 1 $\delta$  $\epsilon$  > r $\alpha$ 1 $\beta$ 1 $\delta$  $\gamma$   $\approx$  h $\alpha$ 3 $\beta$ 2 >> h $\alpha$ 7. Our study emphasizes the importance of loop size and  $\alpha$ -conotoxin sequence specificity for receptor binding. These studies can be used for the evaluation of the neuropharmacology of novel  $\alpha$ -conotoxins that can be utilize as molecular probes for diseases such as, Alzheimer's, Parkinson's, and cancer.

**KEYWORDS:** *venom, cone snails,  $\alpha$ -conotoxins, nAChRs, giant fiber system, Drosophila, oocytes*

**ABBREVIATIONS:** HPLC, high performance liquid chromatography; GF, giant fiber; GFS, giant fiber system; DLM, dorsal longitudinal muscle; nAChR, nicotinic acetylcholine receptor

## 1. INTRODUCTION

Predatory marine mollusks of the genus *Conus* (cone snails) produce a potent and complex venom, largely composed of highly modified peptides (conopeptides and conotoxins) that interact with a variety of molecular targets within their prey such as, K<sup>+</sup> channels, Na<sup>+</sup> channels, Ca<sup>2+</sup> channels, and nicotinic acetylcholine receptors (nAChRs), among others (Akondi et al., 2014; Lewis et al., 2012; Marí and Tytgat, 2010). The venom of each *Conus* species contains over 2,000 unique conopeptides spanning over 30 conotoxin gene superfamilies (Biass et al., 2009; Robinson and Norton, 2014). There are seven classes of conotoxins that target nAChRs (Lebbe et al., 2014). However,  $\alpha$ -conotoxins are the quintessential nAChR inhibitors found in the venom of most species of cone snails (Akondi et al., 2014). These peptides are 12-19 amino acids in length with two loops formed by the cysteine arrangement of C1-C3 and C2-C4 forming disulfide bonds (McIntosh et al., 1999). Several  $\alpha$ -conotoxins are used as molecular probes to inhibit nAChRs with preferential inhibition towards specific subtypes depending upon the  $\alpha$ -conotoxin in question (Cuny et al., 2017; Heghinian et al., 2015). Such specificity has greatly advanced our knowledge of cholinergic-mediated mechanisms of neurological conditions such as Alzheimer's disease, schizophrenia, nicotine addiction, and depression disorders (Taly and Charon, 2012; Valles and Barrantes, 2012; Quik et al., 2015). One  $\alpha$ -conotoxin, Vc1.1, has reached phase IIA clinical trials as a neuropathic pain therapeutic (Castro et al., 2017; Livett et al., 2006).

The fruit fly is an ideal model organism for studying conotoxins due to the small amounts of venom necessary to elicit responses and the extensive number of studies that have been carried out on the neurobiology of these flies. We have previously described a novel bioassay to characterize conotoxins by pairing the *in vivo* nanoinjection of the conotoxins with simultaneous collection of electrophysiological recordings from the *Drosophila melanogaster* giant fiber system (GFS) (Mejia et al., 2010; Mejia et al., 2012). The GFS is a well-characterized neuronal circuit responsible for the mediation of the fly's escape response. The circuit terminating on two muscles, the Dorsal Longitudinal Muscle (DLM) and the Tergo Trochanteral Muscle (TTM), contains three types of neurons with respect to synaptic transmission. The Giant Fiber (GF) innervates the Tergo Trochanteral Motor neuron (TTMn) and the Peripheral Synapsing Interneuron (PSI) via mixed electrical and cholinergic chemical synapses but the connections are predominantly dependent on gap junctions. In contrast, the synapse between the PSI and Dorsal Longitudinal Motor neuron (DLMn) is solely dependent upon the *Drosophila*  $\alpha 7$  nAChR (Heghinian et al., 2015), a homolog of the human  $\alpha 7$  nAChR (Fayyazuddin et al., 2006), whereas the motor neurons use glutamate as a neurotransmitter.

We have previously demonstrated selective disruption of the GF-DLM but not the TTM pathway by several  $\alpha$ -conotoxins from different *Conus* species confirming that this assay is an effective

and specific screening method for  $\alpha$ -conotoxins (Mejia et al., 2013). Here we report the isolation of one known  $\alpha$ -conotoxin (PIA) and two novel  $\alpha$ -conotoxins (PIC and PIC[O7]) and their direct *in vivo* characterization in the *D. melanogaster* GFS. We also determined the activity of PIC and PIC[O7] at rodent and human nAChR subtypes and PIA at human  $\alpha 7$  nAChRs expressed in *Xenopus laevis* oocytes. All three  $\alpha$ -conotoxins were isolated from the injected venom of *Conus purpurascens*, the only fish-hunting cone snail species found in the tropical Eastern Pacific region. The  $\alpha$ -conotoxins of *C. purpurascens* act synergistically with other paralytic components (the motor cabal) to produce a flaccid paralysis as part of the mechanism of envenomation used to secure the prey. The disruption of cholinergic pathways is central to the mechanism of envenomation used by cone snails. Their associated neuropharmacology is still unraveling.

## 2. METHODS AND MATERIALS

### 2.1 Conotoxin extraction

The injected venom was “milked” from a single live *C. purpurascens* individual using the protocol established previously (Hopkins et al., 1995). Briefly, the snail was enticed with a feeder gold fish until the proboscis was extended, and then the fish was replaced with a “trap” made from a microcentrifuge tube with the opening covered in latex and a fish tail. The snail was able to sense the fish tail and sting the trap, injecting its venom into the microcentrifuge tube. The care and maintenance of the gold fish followed the Institutional Animal Care and Use Committee (IACUC) guidelines established at Florida Atlantic University. The injected venom was collected once a week with an average volume of 10  $\mu$ L and stored at  $-80^{\circ}\text{C}$  until needed.

### 2.2 Isolation of Conotoxins by RP-HPLC

PIA, PIC, and PIC[O7] were isolated by RP-HPLC from the injected venom of a single *C. purpurascens* individual (Figure 1) by pooling the venom from several “milkings” to obtain a total volume of 50  $\mu$ L. The venom was then diluted with 0.1% TFA (trifluoroacetic acid) in preparation for RP-HPLC analysis by a Series 200 LC pump (Perkin Elmer, Waltham, MA, USA) coupled to a SpectroMonitor 5000 Photodiode Array Detector (LDC Inc., Carlsbad, CA, USA). Venom was separated on a 4.6 mm x 50 mm, 2.6  $\mu$ m-particle diameter, 100  $\text{\AA}$ -pore size Kinetex C8 column (Phenomenex, Torrance, CA, USA) using an incremental linear gradient of 100% solution A (0.1% TFA, 99.9%  $\text{H}_2\text{O}$ ) to 100% solution B (60% acetonitrile in 0.1% TFA) over 100 min with a flow rate of 1.0 mL/min. Chromatography was monitored using PeakSimple 4.35 system (SRI Instruments, Torrance, CA, USA). Fractions were manually collected under UV monitoring at  $\lambda = 205, 220, \text{ and } 280 \text{ nm}$ . Fractions were dried and stored at  $-20^{\circ}\text{C}$  until needed.

The molecular masses of the conotoxins were determined by MALDI-TOF MS, Applied Biosystems Voyager-DE PRO mass spectrometer (Framingham, MA, USA) (Table 1)(Rodriguez et al., 2015).

### 2.3 Conotoxin Sequencing by Edman degradation

An aliquot corresponding to PIC and PIC[O7] fractions were dried, re-dissolved in 0.1 M Tris-HCl (pH 6.2), 5 mM EDTA, and 0.1 % sodium azide, and reduced with 6 mM dithiothreitol. Following incubation at 60 °C for 30 min, the sample was alkylated in a final volume of 15 µL with 20 mM iodoacetamide and 2 µl of NH<sub>4</sub>OH (pH 10.5) at room temperature (20-24°C) for 1 h in the dark. The reduced/alkylated peptides were dried and re-dissolved in 15 µL of water for sequencing by Edman degradation on an Applied Biosystems Procise model 491A sequencer.

### 2.4 In vivo Electrophysiology in the *Drosophila melanogaster* Giant Fiber

The paired method of electrophysiology and nanoinjection in *D. melanogaster* has been described previously (Mejia et al., 2012; Mejia et al., 2013). Briefly, wild-type flies (*w*<sup>1118</sup>, fly stocks #3605 obtained from the Bloomington Drosophila Stock Center) were kept at 25°C in vials with standard media. The α-conotoxins were prepared in 0.7% saline to a final concentration that allowed for the desired pmol of peptide to be injected. α-Conotoxins PIA, PIC, and PIC[O7] were injected at various concentrations into the hemolymph of the fly while simultaneously recording from the GFS. Control flies were injected with 0.7% saline solution without peptide. The GFs were stimulated in the brain with 10 trains of 10 stimuli given at 100 Hz with 1 s intervals between trains and the GF-DLM and GF-TTM pathways were monitored for changes in the following frequency (FF). Muscle response was monitored before and 1, 5, 10, 15, and 20 min after injection (n = 10 for all experiments). Sigma Plot (Systat Software, San Jose, CA, USA) was used to perform the statistical analysis using a nonparametric Kruskal-Wallis 1-way ANOVA and Tukey test.

### 2.5 In vitro Electrophysiology in *Xenopus* oocytes expressing nAChRs

Oocyte preparation and nAChR subunit expression in *Xenopus* oocytes were performed as described previously (Heghinian et al., 2015). Briefly, plasmids with cDNA encoding the rat (α1, β1, γ and δ), mouse (ε) and human (α7, α3 and β2) nAChR subunits were linearized for *in vitro* mRNA synthesis using mMACHINE kit (Ambion, Foster City, CA, USA). Oocytes were injected with 5 ng cRNA two to five days before recording and kept at 18 °C in ND96 buffer (96 mM NaCl, 2 mM KCl, 1 mM CaCl<sub>2</sub>, 1 mM MgCl<sub>2</sub> and 5 mM HEPES, at pH 7.4) supplemented with 5% fetal bovine serum (Bovogen Biologicals, East Keilor, VIC, Australia), 50 mg/L gentamycin (GIBCO, Grand Island, NY, USA) and 10,000 U/mL penicillin-streptomycin (GIBCO, Grand Island, NY, USA). Voltage-recording and current-injecting microelectrodes were pulled from GC150T-

7.5 borosilicate glass (Harvard Apparatus Ltd., Holliston, MA, USA) giving tip resistances of 0.3–1.5 M $\Omega$  when filled with 3 M KCl. Two-electrode voltage clamp recordings from oocytes were conducted at room temperature (22–23°C) using a GeneClamp 500B amplifier, Digidata 1322A interface and pClamp 9 software (Molecular Devices, Sunnyvale, CA, USA) at a holding potential of –80 mV.

Initially, oocytes in a 10  $\mu$ L recording chamber were continuously perfused with ND96 solution at 2 ml/min, applied by a pump perfusion system. nAChR-mediated currents were evoked by applications of acetylcholine (ACh) at half-maximal effective concentration ( $EC_{50}$ ) of 1  $\mu$ M for rodent muscle, 6  $\mu$ M for  $\alpha 3\beta 2$  and 100  $\mu$ M for  $\alpha 7$  nAChRs. Oocytes were preincubated with peptide for 5 min with the perfusion system turned off, followed by co-application of ACh and peptide with flowing bath solution. Washout with bath solution occurred for 3 min between ACh applications. All peptide solutions were prepared in ND96 + 0.1% bovine serum albumin. Peak ACh-evoked current amplitudes before (ACh alone) and after (ACh + peptide) peptide incubation were measured using Clampfit version 10.7.0.3 software (Molecular Devices, Sunnyvale, CA, USA), where the ratio of ACh + peptide-evoked current amplitude to ACh alone-evoked current amplitude was used to assess the activity of PIA, PIC and PIC[O7] on ACh-evoked currents. All electrophysiological data were pooled and represent means  $\pm$  standard error of the mean (SEM). Data sets were compared using an unpaired Student's t-test (GraphPad Prism 7, GraphPad Software, La Jolla, CA, USA). Differences were regarded statistically significant when  $p < 0.05$ .

### *2.6 Homology Modeling of PIA Bound to the $\alpha 7$ nAChR Receptor*

Homology modeling of PIA and PIC bound to the  $\alpha 7$  nAChR were done with Modeler v9.18 (Webb and Sali, 2014) using a method described previously (Heghinian et al., 2015). Briefly, the X-ray crystal structure of *Aplysia californica* acetylcholine binding protein (AChBP) bound to  $\alpha$ -conotoxin Iml (PDB ID: 2C9T) was used as a binding template (Ulens et al., 2006). Chimera v.6.1 was used for the molecular graphics analysis (Yang et al., 2012).

### *2.7 Transcriptome of the *C. purpurascens* venom duct*

RNA was extracted from freshly dissected venom duct tissue and prepared utilizing the Illumina PolyA-Truseq preparation protocol. Samples were then sequenced on a Next-Seq 500 Illumina sequencing platform to produce four sets of paired end sequences. All runs were concatenated to produce two single independent datasets containing 31 million forward and reverse reads. Quality metrics were obtained using FASTQC and read distribution statistics were calculated with BBMap to prove accurate group fragment pair distance (141 bp) for read assembly. The paired-end data was then assembled using De-Bruijn graph based De Novo assembler, Trinity (Grabherr et al., 2011), to produce a final FASTA dataset containing 64321 independent

assembled contigs. Final assembled contigs were then converted to a BLAST database using NCBI Blast+ and full protein sequences were identified using local NCBI BLASTx with an e-value cutoff of  $e^{-7}$ .

### 3. RESULTS

#### 3.1 Isolation and Sequencing of PIA, PIC and PIC[O7]

The RP-HPLC profile of the injected venom from a single individual of *C. purpurascens* is shown in Figure 1. The peaks eluted at 17 (PIC[O7]), 19 (PIC) and 57 (PIA) min were collected and MALDI-TOF mass spectrometry of the purified RP-HPLC fraction in reflector mode yielded molecular mass of 1460.13, 1475.11 and 1980.94 Da, respectively (Table 1). The theoretical molecular mass of PIA is 1732.42 Da. The fractions that eluted at 17 and 19 min were reduced and alkylated and sequenced using Edman degradation yielding the sequences of the novel  $\alpha$ 4/4-conotoxins PIC and PIC[O7], respectively. The transcriptome of *C. purpurascens* venom revealed the presence of the precursor sequence for PIC and PIC[O7], whose signal sequence corresponds to the A-superfamily of conotoxins (Table 1S).

#### Figure 1

#### 3.2 *In vivo* Electrophysiology Responses of PIA, PIC and PIC[O7] in the *Drosophila melanogaster* Giant Fiber

$\alpha$ -Conotoxins PIA had an inhibitory effect on the GF-DLM pathway (Figure 2A and 2B,  $n = 10$ ). PIA displayed the most significant disruption of the GF-DLM responses at 88 pmol/fly (Figure 2A) compared to the 0.7% saline control injection while having no effect on the GF-TTM pathway (Figure 1S). At this concentration,  $\alpha$ -PIA decreases the probability of DLM responses to  $9.8 \pm 4.4\%$  and  $4.2 \pm 0.2\%$  at 10 and 20 min post injection, respectively. To determine the effects of  $\alpha$ -PIA at lower concentrations, 67, 44, and 21 pmol of PIA/fly were injected as well, which caused a reduced dose-dependent inhibition of the GF-DLM pathway. At the lowest concentration tested, the DLM response probability was reduced to  $67.7 \pm 11.8\%$  by 10 min and  $47.0 \pm 8.0\%$  by 20 min post injection.

PIC caused less inhibition of the GF-DLM pathway at 88 pmol/fly than PIA. Although PIC caused the DLM response to decrease to  $69.5 \pm 16.5\%$  after 20 min post-injection when compared to the 0.7% saline control, an ANOVA analysis followed by a Tukey test showed that these measurements were not statistically significant when compared to the control. PIC[O7] at a concentration of 88 pmol/fly, exhibited no significant inhibition of the DLM response



probability. Similar to  $\alpha$ -PIA, the GF-TTM pathway was unaffected by both, PIC and PIC[O7] (Figure 1S).

## Figure 2

### 3.3 *In vitro* Electrophysiology Activity of PIC and PIC[O7] at Heterologously Expressed nAChRs in *Xenopus* Oocytes

$\alpha$ -Conotoxins PIC and PIC[O7] were tested at vertebrate human (h) $\alpha$ 3 $\beta$ 2, h $\alpha$ 7, rodent (r) $\alpha$ 1 $\beta$ 1 $\delta$  $\gamma$ , and r $\alpha$ 1 $\beta$ 1 $\delta$  $\epsilon$  nAChR subtypes. PIA was tested at the h $\alpha$ 7 nAChR using lml as a positive control. We investigated the effects of the  $\alpha$ -conotoxins on ACh-evoked currents mediated by nAChR subunit combinations expressed in *Xenopus* oocytes (Figure 3A and B). At 1  $\mu$ M,  $\alpha$ -conotoxins PIC and PIC[O7] reversibly inhibited ACh-evoked currents mediated by r $\alpha$ 1 $\beta$ 1 $\delta$  $\epsilon$  nAChR by  $59.8 \pm 7.7\%$  and  $64.1 \pm 4.6\%$  ( $n = 3$ ), respectively. Both conotoxins also inhibited the h $\alpha$ 3 $\beta$ 2 and r $\alpha$ 1 $\beta$ 1 $\gamma$  $\delta$  nAChR subtypes by  $\sim 30$ - $45\%$  whereas, only minimal inhibition ( $<10\%$ ) was observed at the h $\alpha$ 7 nAChR subtype. At 1  $\mu$ M,  $\alpha$ -conotoxin PIA reversibly inhibited h $\alpha$ 7 mediated ACh-evoked currents by  $<5\%$  ( $n = 4$ ), whereas,  $\alpha$ -conotoxin lml, used as a positive control on the same oocytes and at the same concentration, reversibly inhibited  $>80\%$  ( $82.7 \pm 2.2\%$ ,  $n = 4$ ) of ACh-evoked current amplitude. In summary, PIC and PIC[O7] inhibited the muscle and neuronal nAChRs with the following selectivity sequence: r $\alpha$ 1 $\beta$ 1 $\delta$  $\epsilon$   $>$  r $\alpha$ 1 $\beta$ 1 $\delta$  $\gamma$   $\approx$  h $\alpha$ 3 $\beta$ 2  $\gg$  h $\alpha$ 7 (Table 1). Surprisingly, PIC[O7] caused a slightly greater inhibition of r $\alpha$ 1 $\beta$ 1 $\delta$  $\epsilon$  and r $\alpha$ 1 $\beta$ 1 $\delta$  $\gamma$  than PIC.

## Figure 3

### 3.4 Molecular Interactions of PIA and PIC at the D $\alpha$ 7 nAChR

The interactions between PIA, PIC and the D $\alpha$ 7 nAChR were further rationalized by homology modeling based upon the crystal structure of *Aplysia californica* AChBP bound to  $\alpha$ -conotoxin lml (Brejc et al., 2001; Ulens et al., 2006), a suitable surrogate to study nAChR-conotoxin interactions. The key residues of PIA that determine binding to D $\alpha$ 7 nAChR are predicted to be Asn7 and Val9 at the D $\alpha$ 7 principal side, and Ser6 and Val12 at the D $\alpha$ 7 complementary side of the binding pocket. These residues are predicted to bind to the receptor primarily through hydrogen bonding (Figure 4A, red) and hydrophobic interactions (Figure 4A, orange). This model predicts that PIA (yellow) is essentially 'glued' to the interfaces of D $\alpha$ 7 at the C-loop of the principal side (Figure 4A, light blue) and binding pocket of the complementary side (Figure 4A, dark blue). The homology model of PIC and D $\alpha$ 7 predicts fewer conotoxin-receptor

interactions (Fig. 4B), only one interaction with the C-loop of the principal side through R13 in PIC. Additional residues of PIC that determine binding to D $\alpha$ 7 are predicted to be Pro7 at the D $\alpha$ 7 principal side, and Lys11 at the D $\alpha$ 7 complementary side of the binding pocket.

#### Figure 4

#### 4. DISCUSSION

The injected predatory venom of cone snails is a complex mixture of components that act synergistically to immobilize the prey. The functional characterization of such components is a major challenge, as these components are expressed in minute quantities and their direct neuropharmacological assessment, especially when using *in vivo* assays, is typically unreachable. Nevertheless, we have devised a *Drosophila*-based *in vivo* assay that permits the evaluation of picomole venom quantities. This assay is particularly suitable for the characterization of  $\alpha$ -conotoxins, as the GF-DLM pathway (flight response) and not the GF-TTM (jump response) will be affected by  $\alpha$ -conotoxins. Interestingly, not all  $\alpha$ -conotoxins affect the *Drosophila*  $\alpha$ 7 nAChR in the same manner, as we have recently demonstrated for a panel of  $\alpha$ -conotoxins from different species (Heghinian et al., 2015; Mejia et al., 2010; Mejia et al., 2013).

Cone snails express a variety of  $\alpha$ -conotoxins that in turn have can have differential inhibition profiles for the nAChRs present in the prey. The particular individual of *C. purpurascens* analyzed here expresses the known  $\alpha$ 4/7-conotoxin PIA and two new ones, PIC and its hydroxylated analog PIC[O7]. PIC and PIC[O7] are  $\alpha$ 4/4-conotoxins with four amino acid residues between each cysteine loop. This is the same cysteine loop arrangement as PIB (Table 1), a known inhibitor of muscle-subtype nAChRs located at the mammalian neuromuscular junction (Lopez-Vera et al., 2007).  $\alpha$ -PIB was not expressed in the venom of this individual and was not tested. Sequence homology suggests that  $\alpha$ -PIC and  $\alpha$ -PIC[O7] may have similar selectivity to nAChRs as PIB.

Testing of the  $\alpha$ 4/4-conotoxins PIC and PIC[O7] at nAChR subtypes expressed in *Xenopus* oocytes showed that these conotoxins preferentially inhibit the rodent muscle nAChRs more than the human neuronal nAChR subtypes (see Fig. 3). This explains the lack of PIC and PIC[O7] activity at the neuronal nAChRs compared to  $\alpha$ -PIA, a known neuronal nAChR subtype inhibitor. The D $\alpha$ 7 nAChR is a “neuronal-like” subtype, most similar to the mammalian  $\alpha$ 7 subtype (Heghinian et al., 2015). However, D $\alpha$ 7 has been sensitive to most  $\alpha$ -conotoxins tested to date.

These two lineages of  $\alpha$ -conotoxins from the venom of *C. purpurascens* with varying activity between neuronal and neuromuscular nAChRs may partially explain the lower potency of PIC for the D $\alpha$ 7 nAChR when compared to PIA. PIA is a  $\alpha$ 4/7-conotoxin with low sequence homology to the 4/4 counterparts and the longer second loop may be the cause of the difference in selectivity towards the D $\alpha$ 7 nAChR (Cuny et al., 2016). Synthetic  $\alpha$ -PIA does not inhibit human  $\alpha$ 1 $\beta$ 1 $\delta$  $\epsilon$  and it has low selectivity towards rat  $\alpha$ 3 $\beta$ 2 nAChRs when compared to  $\alpha$ 6 $\beta$ 2 $\beta$ 3 (Dowell et al., 2003). In this study, we show that native PIA was inactive at the human  $\alpha$ 7 nAChR. Synthetic conotoxins may exhibit different folding patterns and posttranslational modifications from the native peptide, which could account for differences in sensitivity and activity (Kang et al., 2007; Khoo et al., 2012). It is important to note that in this study we evaluate the *in vivo* activity of conotoxins, which may differ from their activity in single cells.

The nAChR C-loop is essential in linking the conformational changes that occur when the endogenous acetylcholine ligand binds to the receptor to the open the pore. Homology models of the complex between D $\alpha$ 7 and PIA predict multiple interactions at the principal and complementary binding sites that resulted in locking the C-loop in a resting position hindering ACh binding and hampering the conformational changes needed for the channel to open (Celie et al., 2005). As a result, synaptic transmission is inhibited leading to reduced DLM response. In contrast, the model of complex between D $\alpha$ 7 and PIC showed diminished interactions between PIC and the C-loop, which is consistent with PIC non-inhibitory activity when compared to PIA. While these models provide a rationale for such interactions, the precise interaction of conotoxins with nAChRs can vary depending on the specific nAChR subtype and specific conotoxin in consideration.

This study accounts for the efficacious application of the GFS assay, where injected venom components of *C. purpurascens* were used to complete the *in vivo* assay. Here we have described the isolation of picomole quantities  $\alpha$ -conotoxins PIA, PIC, and PIC[O7] from the injected venom of a single individual of *C. purpurascens* and the corresponding *in vivo* functional characterization in a *Drosophila*-based functional assay that involves the D $\alpha$ 7 nAChR subtype. PIA is a known selective  $\alpha$ 6 $\beta$ 2 $\beta$ 3 and to a lesser extent a  $\alpha$ 3 $\beta$ 2 nAChR inhibitor, but we have shown that PIA also inhibits the D $\alpha$ 7 nAChR. We have also shown that the novel  $\alpha$ -conotoxin PIC and its hydroxylated counterpart PIC[O7] have no significant inhibitory activity at D $\alpha$ 7 nAChRs. At  $\alpha$ 1 $\beta$ 1 $\delta$  $\epsilon$  and  $\alpha$ 1 $\beta$ 1 $\gamma$  $\delta$  nAChRs, PIC[O7] is a slightly more potent inhibitor than PIC suggesting that proline hydroxylation plays a delicate role in the mechanism of nAChR inhibition by  $\alpha$ -conotoxins (Franco & Mari, 2005).

We have demonstrated that the *Drosophila*-based *in vivo* assay can be used to functionally characterize minute quantities of  $\alpha$ -conotoxins. These findings can be readily correlated with vertebrate cholinergic pathways (Heghinian et al., 2015; Thany et al., 2007). The GFS assay is an

effective tool for *in vivo* screening of  $\alpha$ -conotoxins, with the advantage of using picomole quantities of the native natural product inhibitors. Furthermore, future studies can be envisioned through genetic manipulations of the D $\alpha$ 7 nAChR, allowing structure-activity relationship studies for  $\alpha$ -conotoxins and nAChR subtypes, which ultimately can be used for the evaluation of the neuropharmacology of novel  $\alpha$ -conotoxins that can be utilized as molecular probes for diseases such as Alzheimer's, Parkinson's, and cancer.

## **DISCLAIMER**

Certain commercial equipment, instruments, or materials are identified in this paper in order to specify the experimental procedure adequately. Such identification is not intended to imply recommendation or endorsement by the National Institute of Standards and Technology, nor is it intended to imply that the materials or equipment identified are necessarily the best available for the purpose.

## **FUNDING SOURCES**

This work was funded by the U.S. National Institutes of Health and the National Institute of Neurological Disorders and Stroke Grant R21NS06637 (to F.M. and T.A.G.) and the Australian Research Council (Discovery Project Grant DP150103990 to D.J.A.).

## **NOTES**

The authors declare no competing financial interest.

## **ACKNOWLEDGMENTS**

We thank Carolina Möller and Nicole Vanderweit (FAU) for their help with collecting the injected venom from *C. purpurascens*. We thank Jared Ragland (NIST) for his help with the statistical analysis of the data.

## REFERENCES

- Akondi, K. B., Muttenthaler, M., Dutertre, S., Kaas, Q., Craik, D. J., Lewis, R. J., Alewood, P. F., 2014. Discovery, synthesis, and structure-activity relationships of conotoxins. *Chem Rev* 114, 5815-5847.
- Biaass, D., Dutertre, S., Gerbault, A., Menou, J. L., Offord, R., Favreau, P., Stocklin, R., 2009. Comparative proteomic study of the venom of the piscivorous cone snail *Conus consors*. *J Proteomics* 72, 210-218.
- Brejck, K., van Dijk, W. J., Klaassen, R. V., Schuurmans, M., van Der Oost, J., Smit, A. B., Sixma, T. K., 2001. Crystal structure of an ACh-binding protein reveals the ligand-binding domain of nicotinic receptors. *Nature* 411, 269-276.
- Castro, J., Harrington, A. M., Garcia-Caraballo, S., Maddern, J., Grundy, L., Zhang, J., Page, G., Miller, P. E., Craik, D. J., Adams, D. J., Brierley, S. M., 2017.  $\alpha$ -Conotoxin Vc1.1 inhibits human dorsal root ganglion neuroexcitability and mouse colonic nociception via GABA<sub>B</sub> receptors. *Gut* 66, 1083-1094.
- Celie, P. H., Kasheverov, I. E., Mordvintsev, D. Y., Hogg, R. C., van Nierop, P., van Elk, R., van Rossum-Fikkert, S. E., Zhmak, M. N., Bertrand, D., Tsetlin, V., Sixma, T. K., Smit, A. B., 2005. Crystal structure of nicotinic acetylcholine receptor homolog AChBP in complex with an  $\alpha$ -conotoxin PnIA variant. *Nat Struct Mol Biol* 12, 582-588.
- Cuny, H., Kompella, S. N., Tae, H. S., Yu, R., Adams, D. J., 2016. Key structural determinants in the agonist binding loops of human  $\beta$ 2 and  $\beta$ 4 nicotinic acetylcholine receptor subunits contribute to  $\alpha$ 3 $\beta$ 4 subtype selectivity of  $\alpha$ -conotoxins. *J Biol Chem* 291, 23779-23792.
- Cuny, H., Yu, R., Tae, H-S., Kompella, S. N., Adams, D. J., 2017.  $\alpha$ -Conotoxins active at  $\alpha$ 3-containing nicotinic acetylcholine receptors and their molecular determinants for selective inhibition. *Br J Pharmacol.* (doi: 10.1111/bph.13852)
- Dowell, C., Olivera, B. M., Garrett, J. E., Staheli, S. T., Watkins, M., Kuryatov, A., Yoshikami, D., Lindstrom, J. M., McIntosh, J. M., 2003.  $\alpha$ -Conotoxin PIA is selective for  $\alpha$ 6 subunit-containing nicotinic acetylcholine receptors. *J Neurosci* 23, 8445-8452.
- Fayyazuddin, A., Zaheer, M. A., Hiesinger, P. R., Bellen, H. J., 2006. The nicotinic acetylcholine receptor  $D\alpha$ 7 is required for an escape behavior in *Drosophila*. *PLoS Biol* 4, e63.
- Grabherr, M. G., Haas, B. J., Yassour, M., Levin, J. Z., Thompson, D. A., Amit, I., Adiconis, X., Fan, L., Raychowdhury, R., Zeng, Q., Chen, Z., Mauceli, E., Hacohen, N., Gnirke, A., Rhind, N., di Palma, F., Birren, B. W., Nusbaum, C., Lindblad-Toh, K., Friedman, N., Regev, A., 2011. Full-length transcriptome assembly from RNA-Seq data without a reference genome. *Nat Biotech* 29, 644-652.
- Heghinian, M. D., Mejia, M., Adams, D. J., Godenschwege, T. A., Mari, F., 2015. Inhibition of cholinergic pathways in *Drosophila melanogaster* by  $\alpha$ -conotoxins. *FASEB J* 29, 1011-1018.
- Hopkins, C., Grilley, M., Miller, C., Shon, K.-J., Cruz, L. J., Gray, W. R., Dykert, J., Rivier, J., Yoshikami, D., Olivera, B. M., 1995. A new family of *Conus* peptides targeted to the nicotinic acetylcholine receptor. *J Biol Chem* 270, 22361-22367.
- Kang, T. S., Radic, Z., Talley, T. T., Jois, S. D., Taylor, P., Kini, R. M., 2007. Protein folding determinants: structural features determining alternative disulfide pairing in  $\alpha$ - and  $\chi/\lambda$ -conotoxins. *Biochemistry* 46, 3338-3355.

Khoo, K. K., Gupta, K., Green, B. R., Zhang, M. M., Watkins, M., Olivera, B. M., Balaram, P., Yoshikami, D., Bulaj, G., Norton, R. S., 2012. Distinct disulfide isomers of  $\mu$ -conotoxins KIIIA and KIIIB block voltage-gated sodium channels. *Biochemistry* 51, 9826-9835.

Lebbe, E. K., Peigneur, S., Wijesekara, I., Tytgat, J., 2014. Conotoxins targeting nicotinic acetylcholine receptors: an overview. *Mar Drugs* 12, 2970-3004.

Lewis, R. J., Dutertre, S., Vetter, I., Christie, M. J., 2012. *Conus* venom peptide pharmacology. *Pharmacol Rev* 64, 259-298.

Livett, B. G., Sandall, D. W., Keays, D., Down, J., Gayler, K. R., Satkunanathan, N., Khalil, Z., 2006. Therapeutic applications of conotoxins that target the neuronal nicotinic acetylcholine receptor. *Toxicon* 48, 810-829.

Lopez-Vera, E., Jacobsen, R. B., Ellison, M., Olivera, B. M., Teichert, R. W., 2007. A novel  $\alpha$  conotoxin ( $\alpha$ -PIB) isolated from *C. purpurascens* is selective for skeletal muscle nicotinic acetylcholine receptors. *Toxicon* 49, 1193-1199.

Marí, F., Tytgat, J., 2010. 2.15 - Natural Peptide Toxins. *Comprehensive Natural Products II*. Elsevier, Oxford, pp. 511-538.

McIntosh, J. M., Santos, A. D., Olivera, B. M., 1999. *Conus* peptides targeted to specific nicotinic acetylcholine receptor subtypes. *Annu Rev Biochem* 68, 59-88.

Mejia, M., Heghinian, M. D., Busch, A., Armishaw, C. J., Mari, F., Godenschwege, T. A., 2010. A novel approach for in vivo screening of toxins using the *Drosophila* Giant Fiber circuit. *Toxicon* 56, 1398-1407.

Mejia, M., Heghinian, M. D., Busch, A., Mari, F., Godenschwege, T. A., 2012. Paired nanoinjection and electrophysiology assay to screen for bioactivity of compounds using the *Drosophila melanogaster* giant fiber system. *J Vis. Exp.* 62, doi: 10.3791/3597

Mejia, M., Heghinian, M. D., Mari, F., Godenschwege, T. A., 2013. New tools for targeted disruption of cholinergic synaptic transmission in *Drosophila melanogaster*. *PLoS ONE* 8, e64685.

Quik, M., Zhang, D., McGregor, M., Bordia, T., 2015. Alpha7 nicotinic receptors as therapeutic targets for Parkinson's disease. *Biochem Pharmacol* 97, 399-407.

Robinson, S. D., Norton, R. S., 2014. Conotoxin gene superfamilies. *Mar Drugs* 12, 6058-6101.

Rodriguez, A. M., Dutertre, S., Lewis, R. J., Mari, F., 2015. Intraspecific variations in *Conus purpurascens* injected venom using LC/MALDI-TOF-MS and LC-ESI-TripleTOF-MS. *Anal Bioanal Chem* 407, 6105-6116.

Taly, A., Charon, S., 2012.  $\alpha$ 7 nicotinic acetylcholine receptors: a therapeutic target in the structure era. *Curr Drug Targets* 13, 695-706.

Thany, S. H., Lenaers, G., Raymond-Delpech, V., Sattelle, D. B., Lapied, B., 2007. Exploring the pharmacological properties of insect nicotinic acetylcholine receptors. *Trends Pharmacol Sci* 28, 14-22.

Ulens, C., Hogg, R. C., Celie, P. H., Bertrand, D., Tsetlin, V., Smit, A. B., Sixma, T. K., 2006. Structural determinants of selective  $\alpha$ -conotoxin binding to a nicotinic acetylcholine receptor homolog AChBP. *Proc Natl Acad Sci U S A* 103, 3615-3620.

Valles, A. S., Barrantes, F. J., 2012. Chaperoning  $\alpha$ 7 neuronal nicotinic acetylcholine receptors. *Biochim Biophys Acta* 1818, 718-729.

Webb, B., Sali, A., 2014. Protein structure modeling with MODELLER. *Methods Mol Biol* 1137, 1-15.

Yang, Z., Lasker, K., Schneidman-Duhovny, D., Webb, B., Huang, C. C., Pettersen, E. F., Goddard, T. D., Meng, E. C., Sali, A., Ferrin, T. E., 2012. UCSF Chimera, MODELLER, and IMP: an integrated modeling system. *J Struct Biol* 179, 269-278.

**Table 1. Sequences and nAChR selectivity of  $\alpha$ -conotoxins from the venom of *C. purpurascens*.**

Conotoxin	Sequence	Molecular mass (Da)	nAChR selectivity <sup>a</sup>
PIA (Dowell et al., 2003)	RDP <b>CC</b> SNPV <b>CT</b> VHNPQ <b>IC</b> *	1980.94	$r\alpha_6/\alpha_3\beta_2 \geq r\alpha_6/\alpha_3\beta_2\beta_3 > r\alpha_6/\alpha_3\beta_4 > r\alpha_3\beta_2 > r\alpha_3\beta_4 \gg r\alpha_4\beta_2, r\alpha_4\beta_4$  $h\alpha_6/\alpha_3\beta_2\beta_3 > h\alpha_6/\alpha_3\beta_4 \gg h\alpha_1\beta_1\delta\epsilon$
PIB (Lopez-Vera et al., 2007)	ZSOG <b>CC</b> WNPAC-VK <b>NR</b> -- <b>C</b> *	(not in this study)	$r\alpha_1\beta_1\delta\epsilon, r\alpha_1\beta_1\gamma\delta \gg r\alpha_3\beta_2, r\alpha_3\beta_4, r\alpha_7$
PIC	SG <b>CC</b> KHPAC-G <b>KNR</b> -- <b>C</b>	1460.13	$r\alpha_1\beta_1\delta\epsilon > r\alpha_1\beta_1\delta\gamma \approx h\alpha_3\beta_2 \gg h\alpha_7$
PIC[O7]	SG <b>CC</b> KHOAC-G <b>KNR</b> -- <b>C</b>	1475.11	$r\alpha_1\beta_1\delta\epsilon > r\alpha_1\beta_1\delta\gamma \approx h\alpha_3\beta_2 \gg h\alpha_7$

\* indicates an amidated C-terminus, Z indicates pyroglutamate, O indicates hydroxyproline.<sup>a</sup>r = rodent, h = human



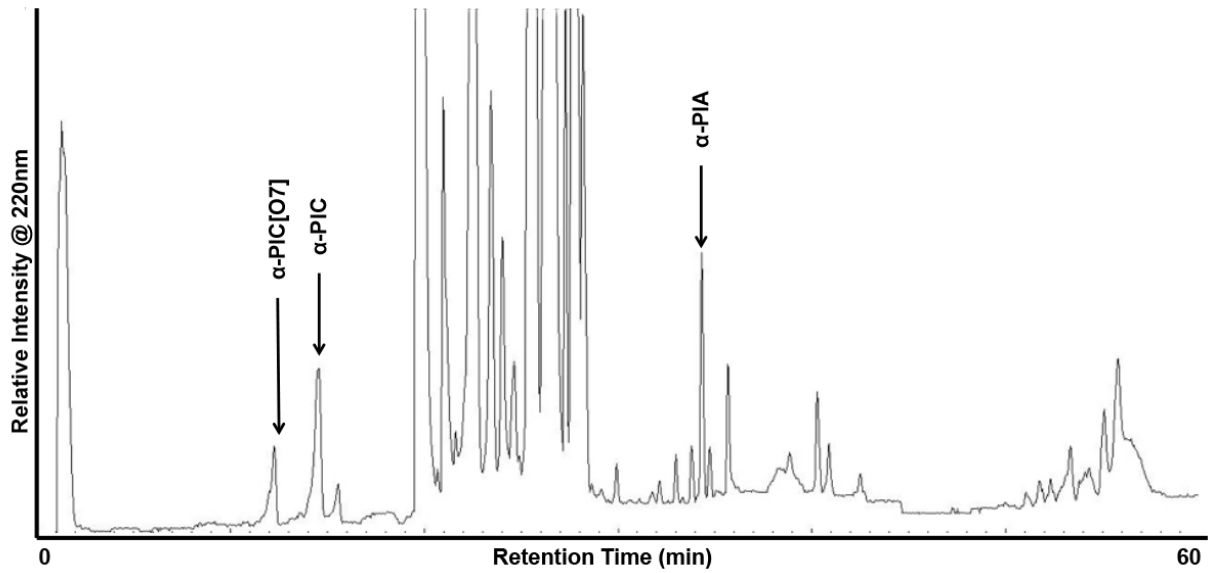


**Figure 1.** Isolation of PIA, PIC, and PIC[O7] by reversed-phase HPLC of the injected venom of a single individual of *C. purpurascens*.

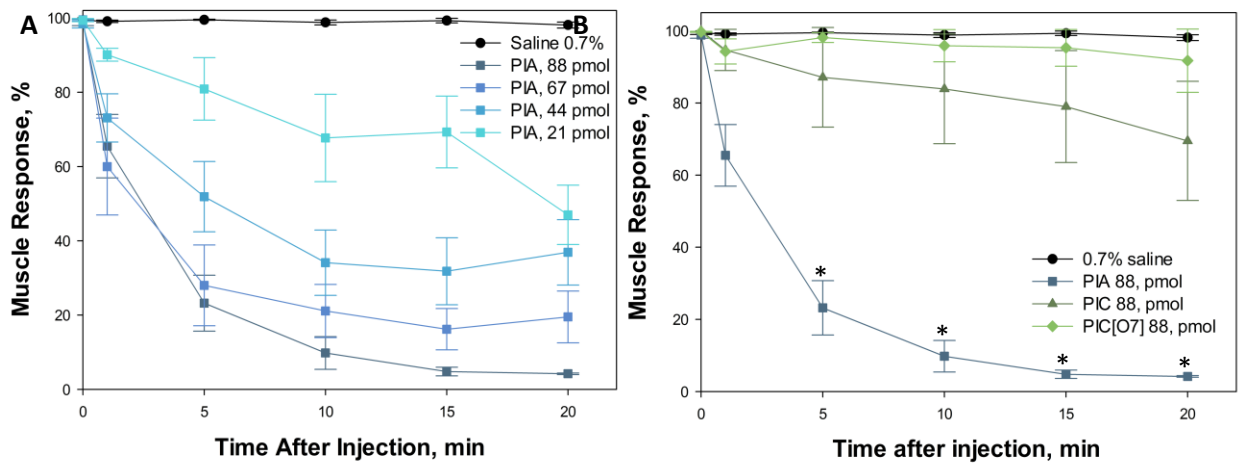


**Figure 2 .** Functional characterization of  $\alpha$ -conotoxins PIA, PIC, and PIC[O7] in picomoles/fly in the *D. melanogaster* giant fiber system (GFS). (A) Effect of PIA at different concentrations on the following frequency (FF) of the GF-DLM pathway. (B) Effect of PIC and PIC[O7] on the FF of the GF-DLM pathway (mean  $\pm$  SEM, n = 10, \*  $p < 0.05$ )

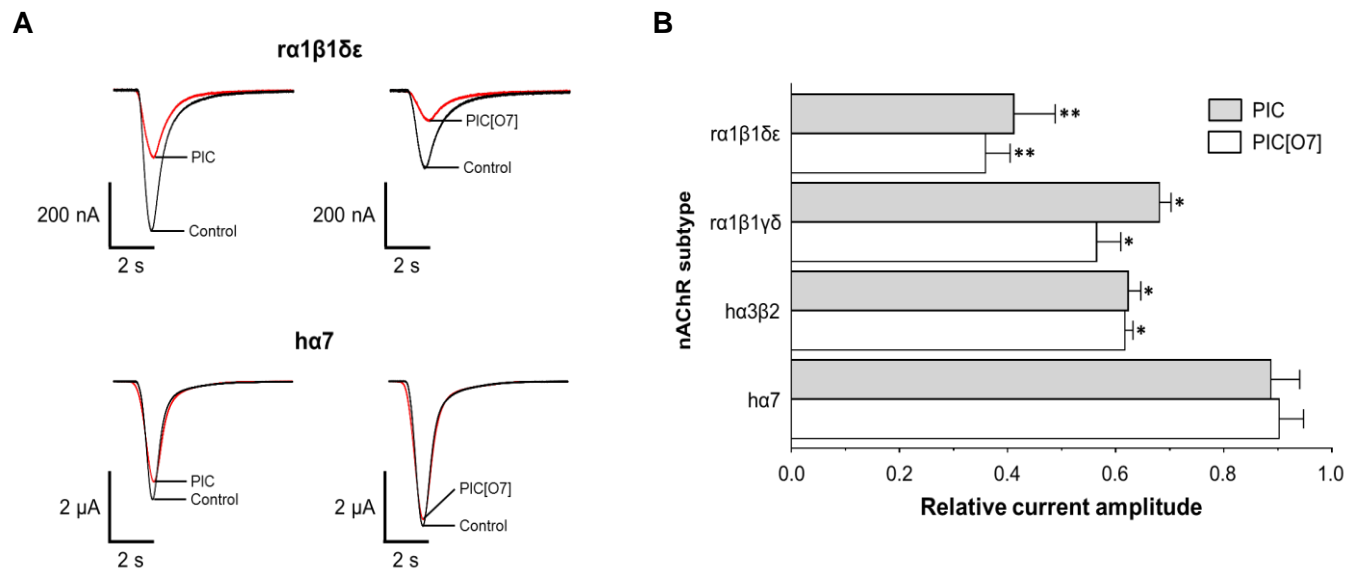
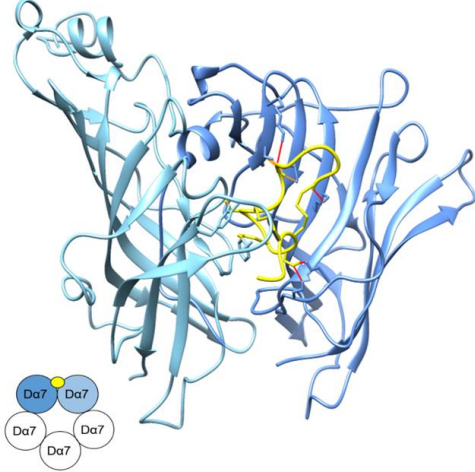
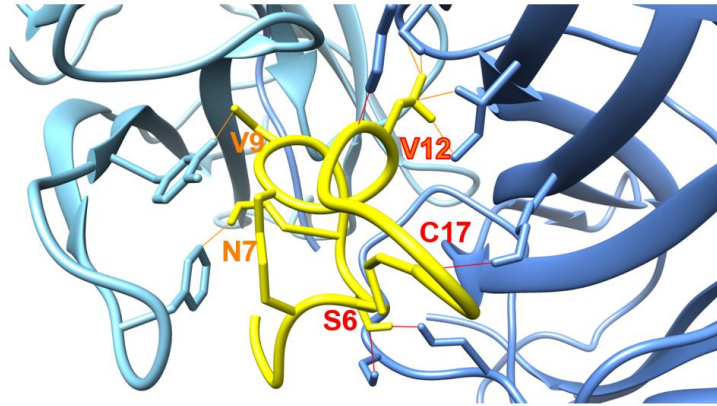


**Figure 3.** Activity of PIC and PIC[O7] at rodent and human nAChR subtypes. A) Superimposed representative ACh-evoked currents recorded from *X. laevis* oocytes expressing rodent ( $r\alpha 1\beta 1\delta\epsilon$ ) and human ( $h\alpha 7$ ) nAChRs in the absence (control, black trace) and presence (red trace) of 1  $\mu$ M PIC or 1  $\mu$ M PIC[O7]. B) Bar graph of PIC and PIC[O7] (1  $\mu$ M) inhibition of ACh-evoked peak current amplitude mediated by  $r\alpha 1\beta 1\delta\epsilon$ ,  $r\alpha 1\beta 1\gamma\delta$ ,  $h\alpha 3\beta 2$  and  $h\alpha 7$  subtypes (mean  $\pm$  SEM,  $n = 3$ , \*  $p < 0.05$ , \*\*  $p < 0.0001$ ).

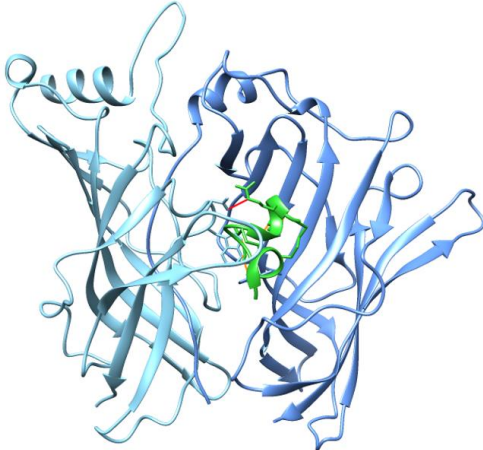
A. PIA-Da7



B. PIA-Da7



C. PIC-Da7



D. PIC-Da7

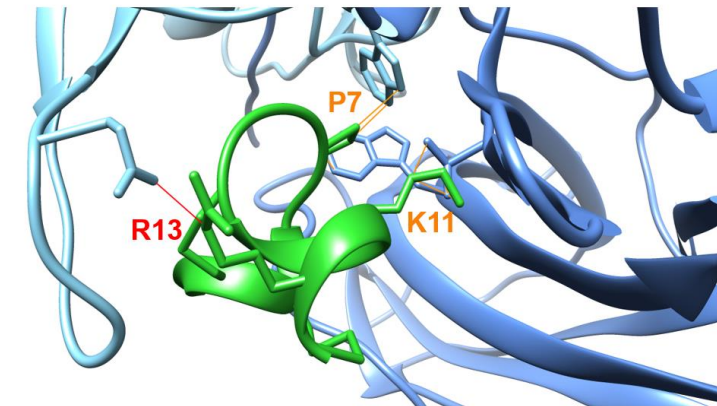


**Figure 4.** **A.** PIA (yellow) bound at the interface of the principal (light blue) and complementary (dark blue) Da7 subunits. Inset: Position of PIA/PIC (yellow) bound between Da7 subunits **B.** PIA is complexed to the binding pocket via hydrogen bond interactions between residues S6, V12 and C17 (red) with the principal binding side and hydrophobic interactions between residues N7 and V9 (orange) with the C-loop of the complementary side. V12 is involved in hydrogen bonding and hydrophobic interactions. **C.** PIC (green) bound at the interface of the principal (light blue) and complementary (dark blue) Da7 subunits. **D.** PIC is complexed to the binding pocket via a single hydrogen bond interactions between residue R13 (red) with the principal binding site and hydrophobic interactions between residue K11 (orange) with the complementary side and P7 (orange) with the principal binding side.